

**COMPUTATIONAL STUDY ON THE EFFECTS OF  
HALOGENATED COMPOUNDS ON AMYLOID-BETA 40  
MONOMER AGGREGATION IN ALZHEIMER'S DISEASE**

A Thesis  
Presented to  
The Academic Faculty

by

Jin Eun Shin

In Partial Fulfillment  
of the Requirements for the Degree  
B.S. in Biomedical Engineering with the Research Option  
in the Wallace H. Coulter School of Biomedical Engineering

Georgia Institute of Technology  
May 2016

**COPYRIGHT 2016 BY JIN EUN SHIN**

**COMPUTATIONAL STUDY ON THE EFFECTS OF  
HALOGENATED COMPOUNDS ON AMYLOID-BETA 40  
MONOMER AGGREGATION IN ALZHEIMER'S DISEASE**

Approved by:

Dr. Seung Soon Jang, Advisor  
School of Materials and Science Engineering  
*Georgia Institute of Technology*

Dr. Anant K. Paravastu, Advisor  
School of Chemical and Biomolecular Engineering  
*Georgia Institute of Technology*

Date Approved: April 20<sup>th</sup>, 2016

## ACKNOWLEDGEMENTS

I wish to thank Dr. Seung Soon Jang, my research principal investigator, who allowed me to work in his lab during my undergraduate semesters. Also, I want to thank Dr. Sang Eun Jee, a postdoctoral researcher in Dr. Jang's lab, for teaching me how to run computational simulations in LINUX OS and helping me solve problems that I face while running simulations. Furthermore, I thank Dr. Anant K. Paravastu who has shown interest in my study and was willing to be the second reader of this thesis. Lastly, I want to thank my colleagues, Hanbyeol Jin et al. who have contributed to this research for a few semesters.

# TABLE OF CONTENTS

	Page
ACKNOWLEDGEMENTS	iii
LIST OF TABLES	vi
LIST OF FIGURES	vii
LIST OF SYMBOLS AND ABBREVIATIONS	viii
SUMMARY	ix
<u>CHAPTER</u>	
1 INTRODUCTION	1
Background	1
Halogenation	1
Literature Review	2
2 MATERIALS AND METHODS	6
Structure Preparation	6
Molecular Docking	7
Molecular Dynamics Simulations	8
Methods of Analysis	9
3 RESULTS	11
Structural Deformation of A $\beta$ <sub>40</sub>	11
Secondary Structure Analysis	12
Root Mean Square Deviation (RMSD) Analysis	13
Minimum Distance Calculations	14
4 DISCUSSIONS	15
Structural Deformation of A $\beta$ <sub>40</sub>	15

Secondary Structure Analysis of A $\beta$ <sub>40</sub>	15
Statistical Analysis for A $\beta$ <sub>40</sub> Conformational Change	16
Distance between Drugs and A $\beta$ <sub>40</sub>	16
5 CONCLUSIONS	18
REFERENCES	19

## LIST OF TABLES

	Page
Table 1: Simulation box dimensions	8
Table 2: Deformation of the Structure of $A\beta_{40}$	11

## LIST OF FIGURES

	Page
Figure 1: Chemical Structures of ER and EOY	6
Figure 2: Most potential binding sites of ER and EOY on A $\beta$ <sub>40</sub>	7
Figure 3: Secondary structure compositions	12
Figure 4: Root mean square deviation of A $\beta$ <sub>40</sub> 's position A $\beta$ <sub>40</sub>	13
Figure 5: Distance between the Drug Molecules and A $\beta$ <sub>40</sub>	14

## LIST OF SYMBOLS AND ABBREVIATIONS

AD	Alzheimer's Disease
ER	Erythrosine B
EOY	Eosin Y
PHB	Phloxine B
ROB	Rose Bengal
FLN	Fluorescein
DSSP	Define Secondary Structures of Protein
RMSD	Root Mean Square Deviation
MD	Molecular Dynamics



## SUMMARY

Alzheimer's disease (AD) is one of the most common types of degenerative dementia. Investigation into the mechanism of aggregation of the most potential Alzheimer's protein, amyloid-beta ( $A\beta_{40}$ ) peptide suggested that the initial  $\alpha$ -helical  $A\beta$  monomer structured transformed into an intermediate state of aggregation. Erythrosine B (ER) is a component of FDA-approved red food dye. Dr. Kwon at University of Virginia observed that the halogenated structure of ER inhibited the formation of  $A\beta$  fibril via *in vitro* experiments. Our group used computational molecular modeling such as AutoDock docking and molecular dynamics simulations to test the effect of ER and its modified version, EOY, on  $A\beta_{40}$  monomer. The drug candidates were modeled using Cerius2, and initial  $A\beta_{40}$  structure was obtained from the protein data bank (ID: 1BA4). AutoDock was used to perform molecular docking, and then molecular dynamics (MD) simulations were conducted using GROMACS 4.6.1 software package. An approximate binding site for each system was found using AutoDock. When the MD simulations were run, the drug molecules were located in the binding sites. Four analysis methods were used to investigate the interactions between  $A\beta_{40}$  and the drug candidates: comparison of the protein structures, secondary structure analysis, root mean square deviation (RMSD) of the protein's position, and distance calculation between  $A\beta_{40}$  and the drug candidates. According to our analyses, ER was effective in preventing the conformational change of  $A\beta_{40}$ , whereas EOY was a relatively poor inhibitor due to weak binding with  $A\beta_{40}$ .

# CHAPTER 1

## INTRODUCTION

### Background

Various human diseases, including some neurodegenerative diseases, have been found to be correlated to conformational transition of specific proteins from their natural forms into insoluble fibrillar forms [1]. Among those diseases, Alzheimer's disease (AD) is known to be the most rampant, age-related dementia [1]. The exact pathological information of AD is still unclear, but many studies have shown that amyloid beta ( $A\beta$ ), a type of neurotoxic protein, plays a crucial role in pathogenesis of AD. The natural  $A\beta$  peptides, which have helical structures, are not harmful; however, once they start to unfold, aggregate, and form fibrils or  $\beta$ -sheet structures, their neurotoxicity increases significantly. Due to this characteristic of  $A\beta$ , many researchers have attempted to discover or develop chemical compounds that can prevent the change in conformation through different approaches.

### Halogenation

Halogenation, a reaction that results from addition of the halogen to a compound, was found to be effective in terms of preventing fibrillogenesis or  $\beta$ -sheet structure formation [2]. Wong, Irwin, and Kwon applied the finding to test the effectiveness of erythrosine B (ERB), a content of red food dye, and its analogues, eosin Y (EOY), phloxine B (PHB), rose Bengal (ROB), and fluorescein (FLN) (negative control) on the  $A\beta$  conformational change via *in vivo* and *in vitro* methods [2]. However, no computational study has been conducted to validate the experimental results. Our research group decided to confirm the abilities of ERB (ER) and EOY, which were chosen to be the most effective chemicals by Wong, Irwin, and Kwon, through

computational molecular dynamics (MD) simulations. We used GROMACS software package and applied AMBER force field for the MD simulations.

Most of the studies in this field have been heavily focused on *in vivo* and *in vitro* tests. For our research group, which specializes in computational methods, those candidates and their modifications could be promising subjects. This research will contribute to improvement of the contents of Alzheimer's drug in terms of accessibility, efficiency, and ultimately efficacy.

### **Literature Review**

Alzheimer's disease (AD) is one of the most common type of age-related dementia [3] that shows symptoms such as memory loss, declined cognitive skills, and sudden change in personality. Despite the amount of research being done, the exact pathological factor is still unclear. Several potential causes have been reported to be correlated to AD. One of the most popular beliefs is that amyloid beta ( $A\beta$ ), a type of neurotoxic protein, plays a crucial role in pathogenesis of AD. According to previous studies, natural  $A\beta$  peptides which have helical structures are not harmful; however, once they start to unfold, aggregate, and form fibrils or  $\beta$ -sheet structures, their neurotoxicity increases significantly. Due to this characteristic of  $A\beta$ , many researchers have attempted to discover or develop chemical compounds that can prevent the conformational change through different approaches. However, because of some uncertainties of its structure and chemical properties, at this moment, it is not even easy to accurately and comprehensively define what  $A\beta$  is [3]. Thus, research is actively ongoing for a better understanding of the AD pathology and developing its novel treatment.

Much effort has been made to understand the functioning of  $A\beta$  as a potentially major cause of AD and investigate its interaction with various drug candidates. Despite

some uncertainties about  $A\beta$ , it has been clear that its formation and aggregation increase neurotoxicity [3], so many studies were conducted to tackle the protein via different approaches. Aquizzi and O'Connor state that mainly three approaches or goals have been taken by researchers—inhibition of enzymatic activities that form  $A\beta$  from its precursor, enhancement of immune system to remove  $A\beta$ , and prevention of  $A\beta$  aggregation [3].

Even though many researchers have the same goal among the three popular ones, they still use different candidate compounds that have unique characteristics that they want to test. For instance, halogenation, a reaction that results in addition of the halogen to a compound, was found to be effective in terms of preventing fibrillogenesis or  $\beta$ -sheet structure formation [4]. Wong, Irwin, and Kwon applied the finding to conduct their research which was to test the effectiveness of erythrosine B (ERB), which contains four iodines and four carbon rings, and its analogues, EOY, PHB, ROB, and FLN on the  $A\beta$  conformational change via *in vivo* and *in vitro* methods [2]. They utilized Thioflavin T fluorescence assay, transmission electron microscopy (TEM), MTT reduction assay and others to test the compounds. ERB and EOY were found to be the most effective compounds [2], but the result has not been further validated in dry-lab environment. Thus, that gap was attractive to our computational research group. Our group is conducting research to investigate the mechanism of interactions between the drug candidates (ERB, EOY and others) and  $A\beta$  monomer via computer simulations using GROMACS and AMBER force field.

Many more studies have been conducted to understand how a compound can be considered effective in terms of preventing  $A\beta$  conformational transition. Li et al. tested their compounds, LRL22, LRL27, K162, and K182, but, uniquely, through computational

means [1]. They examined the compounds to observe their effects on A $\beta$  monomer and oligomer conformational change and their relative effectiveness [1]. They concluded that influential candidates tend to interact with the hydrophobic core I region (residue 17-21) of A $\beta$  monomer which is a favorable result regarding previous studies that discovered those residues' role in promoting A $\beta$  aggregation [1]. In addition, to being an efficient candidate, it should have high binding energy and/or high specificity for the area of interaction (i.e. it must be specific to hydrophobic core I, II or III region) [1]. The drug candidates, however, were only effective for A $\beta$  monomer, but not oligomer [1]. Thus, to some extent, they contributed to establishing criteria for being efficient drug candidates.

Recently, Du et al. proposed another novel way to determine efficiency of drug candidates. They concluded that a drug candidate that can perform “dual function” can be regarded efficient [5]. Brazilin, their test compound, was found to be able to simultaneously perform two functions -- inhibitory and remodeling functions. In other words, brazilin does not only inhibit A $\beta$  conformational change from helical to fibrillar structure, but also destabilize already-mature fibrils to turn into unorganized, less toxic substances [5]. Their finding can be appreciated because it shed light on improving current AD treatments' efficiency and therapeutic capability by having one drug attacking in two different ways.

Despite the fact that most AD research targets A $\beta$  protein, some of the studies investigate other types of proteins as potentially significant causes of AD. For instance, sets of studies were conducted to test drug candidates' effect on cyclooxygenase (COX) [6]. COX level in the microglia and the hippocampus was discovered to increase in AD patients, thus promoting inflammation within the brain [6]. Irannejad et al. validated the

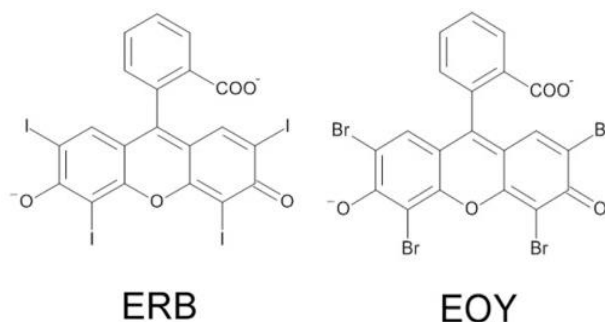
effect of new compound, 1,2-Diaryl-2-hydroxyiminoethanones and its modifications, but the more attractive and important feature about this experiment is to test the compounds' effect on two targets,  $A\beta$  and COX. The paper concludes that the compound with methoxyl for its functional group (R) was the most effective in inhibiting the roles of  $A\beta$  and COX [6].

In conclusion, the attempt to unveil the mysteries about AD pathogenesis and function of its correlated proteins like  $A\beta$  and to investigate the mechanism of protein-drug interaction has been ceaseless. Many of the experiments have been focused on biochemical means to study AD and drug candidates, but relatively fewer studies were done using computational methods. More computer-based molecular dynamics simulations should help researchers overcome some restrictions of wet experiment and provide deeper insight into the mechanisms on molecular level. Another important research gap that needs to be filled is the structure of  $A\beta$  oligomer. Its oligomer is more toxic and problematic than monomer, but yet there is no defined structure for the oligomer for use in computer simulations. Moreover, as shown in Irannejad et al.'s research, there may be more unrevealed factors that are correlated to AD pathology [6]. In spite of the need for more research, analyses of results still need to be thorough and flawless. The current study aims to contribute to the field of AD research by, first, verifying the result of Wong, Irwin, and Kwon's study about halogenation [2] through computational means. This will guide some of the AD researchers to investigate other kinds of halogenated compounds. Potentially, some aspects from halogenation and mechanism of brazilin that allows its dual function can be merged for a stronger and more efficient compound. In the future, we will examine factors that might influence the abilities of the compounds such as their concentrations, pH of the environment, modification of  $A\beta$  and others.

## CHAPTER 2

### MATERIALS AND METHODS

The main goal of this study is to investigate how the two drug candidates, ER and EOY, are able to physically bind to single  $A\beta_{40}$  protein and prevent the deformation of the protein, the precondition of the  $A\beta_{40}$  aggregation. Furthermore, the effects of ER and EOY were compared to investigate the effect of halogen functional group on structural deformation of  $A\beta_{40}$ . As a negative control, we also carried out simulations on  $A\beta_{40}$  without any treatment. Initially, structures of the protein and the drugs were prepared, and the potential binding sites of the drugs on the protein were determined with docking simulations. Then the molecular dynamics simulations were run, which encompass equilibration processes.



**Figure 1. Chemical Structures of ER and EOY**  
doi:10.1371/journal.pone.0057288.g001 [2]

#### Structure Preparation

Molecular structure of  $A\beta_{40}$  monomer was obtained from protein databank (rscb.org. PDB ID: 1BA4) [7]. The structure was extracted from NMR experiments, which maintained its helicity in aqueous micellar environment. Chemical structures of ER and EOY were drawn using Cerius2 software [8], and energy was minimized using steepest descent gradient method to obtain reasonable structure. Then the partial charges of the drug molecules were calculated via ab initio calculations using Jaguar [9] to

describe non-bonded electrostatic interactions. Partial atomic charges of entire atoms were estimated to generate total molecular charges of -2 for both ER and EOY. LACV3P\*\* basis set was used, and spin multiplicity for both compounds was set to 1. Among the calculation options, Mulliken population was chosen to characterize charge distribution throughout each molecule.

### Molecular Docking

Molecular docking between the protein and drug was investigated using AutoDock 1.5.6 docking simulation program [10]. To investigate the energetically stable binding sites for the drugs to  $A\beta_{40}$ , the interaction energy grid was calculated surrounding the protein. Based on center coordinates and dimensions of the energy grid boxes, we performed docking simulations using AutoDock Vina to find the potential binding sites on  $A\beta_{40}$  protein for ER and EOY separately. Nine conformations with the lowest binding energy were calculated for each drug molecule, and the position with the lowest energy was chosen to the most stable binding site. Figure 2 shows the bindings sites for ER- $A\beta_{40}$  and EOY- $A\beta_{40}$  with the estimated binding energy of -1.184 kJ/mol and -1.191 kJ/mol, respectively. After choosing the best binding site for each drug candidate, we made two systems by locating a molecule of ER and EOY near  $A\beta_{40}$  at the specific binding site.



**Figure 2. Most potential binding sites of ER and EOY on  $A\beta_{40}$**  These were results of Autodock docking simulations. (Left) ER- $A\beta_{40}$ . (Right) EOY- $A\beta_{40}$ .



## Molecular Dynamics Simulations

GROMACS 4.6.6 software was used to perform molecular dynamics (MD) simulations. Three systems were examined in this study: A $\beta$ <sub>40</sub> with ER, A $\beta$ <sub>40</sub> with EOY, and A $\beta$ <sub>40</sub> by itself as a negative control. For all the GROMACS simulations, AMBER99SB-ILDN [11] force field was used to accurately describe secondary structures of the protein. To describe ER and EOY, we used DREIDING force field with the estimated electrostatic charges using ab initio calculations as discussed before [12]. Each system was put into the triclinic box whose size was set as shown in Table 1. Then each system was filled with water molecules which were described by simple-point charge (SPC) model [13]. To neutralize the system, 150 mM NaCl was added to the systems.

	x (nm)	y (nm)	z (nm)
A $\beta$ <sub>40</sub> Only	5.67025	3.68988	3.500
A $\beta$ <sub>40</sub> -ER	5.715	3.719	3.620
A $\beta$ <sub>40</sub> -EOY	7.000	7.000	7.000

**Table 1. Simulation box dimensions** Dimensions of simulation boxes for the three systems are listed.

There were four steps to MD simulations, first of which was to minimize the systems' energies in order to make sure the systems were free of steric clashes. Energy minimization was performed applying steepest descent integration method for 50,000 steps. After that, the systems underwent NVT equilibration for 800 ps to stabilize potential, kinetic, and total energies as well as to converge temperature to 310 K. NVT equilibration was followed by equilibration under NPT ensemble for 800 ps, which was to adjust and stabilize the system under constant pressure of 1 bar. During equilibration, the backbone atoms of A $\beta$ <sub>40</sub> were restrained by imposing 1000 kJ/mol of energy per atom. After that, the restraint was released, and the simulations were performed for 150 ns to collect the data. The particle-mesh Ewald method was used to deal with the long-distance

electrostatic interactions. To control the constant temperature and pressure, Berendsen Thermostat and Parrinello-Rahman Barostat were used, respectively. Newton's equation of motion was integrated using Velocity-Verlet algorithm with 2 fs time steps. The simulation results were analyzed with built-in functions of GROMACS.

## Methods of Analysis

### Structural Deformation of A $\beta$ <sub>40</sub>

To investigate the structural deformation of A $\beta$ <sub>40</sub>, we compared structures of the three systems at 0, 50, 100, and 150 ns. The images help us visualize how a protein and a drug interact with each other throughout the simulation. From the images, we would be able to observe whether A $\beta$ <sub>40</sub> undergoes conformational changes from  $\alpha$ -helices to  $\beta$ -structures.

### Secondary Structure Analysis using DSSP

To investigate the effect of the drugs on the deformation of A $\beta$ <sub>40</sub>, secondary structures of A $\beta$ <sub>40</sub> protein in the three systems were analyzed using DSSP [14] throughout the simulation time of 150 ns. DSSP classifies the secondary structures by specifying the hydrogen bonds based on equations presented by Kabsch and Sanders.

DSSP outputs a color map that shows compositions of different secondary structures at forty residues of A $\beta$ <sub>40</sub> over the entire simulation time, 150 ns. Each color represents different kinds of secondary structures such as  $\alpha$ -helix to  $\beta$ -structure.

### Root Mean Square Deviation (RMSD)

Root mean square deviation was used to measure the structural deformation of A $\beta$ <sub>40</sub> in presence of the drugs over simulation time. RMSD is the averaged fluctuations of the atomic positions compared to the reference structures, as shown in equation (2)

$$\text{RMSD} = \sqrt{\frac{1}{N} \sum_{i=1}^N \delta_i^2} = \sqrt{\frac{1}{N} \sum_{i=1}^N [(x_i - x_i^o)^2 + (y_i - y_i^o)^2 + (z_i - z_i^o)^2]} \quad (2)$$

, where  $x_i, y_i, z_i$  represents the x, y, z position at time t and  $x_i^o, y_i^o, z_i^o$  are initial positions of atom  $i$  of total number of atoms, N, respectively. RMSD of A $\beta_{40}$  was estimated from the position of the backbone atoms and fitted to the initial structures. Therefore, high RMSD indicates significant atomistic displacement throughout MD simulation. This means the protein went through conformational changes which require a lot of movement of atoms. Numerical results were expressed as mean  $\pm$  SD.

### **Minimum Distance Calculations**

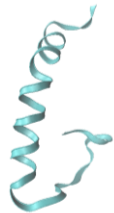

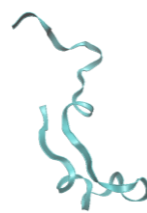
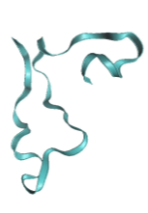





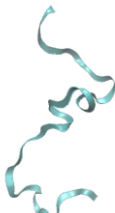


Minimum distance between centers of mass of A $\beta_{40}$  and the drugs was calculated to compare binding affinity of ER and EOY as A $\beta_{40}$  fibrillogenesis inhibitors. The one with lower distance values over the simulation time was considered to interact more with the protein, thus being most likely to be bound more strongly.

## CHAPTER 3

### RESULTS

#### Structural Deformation of A $\beta_{40}$

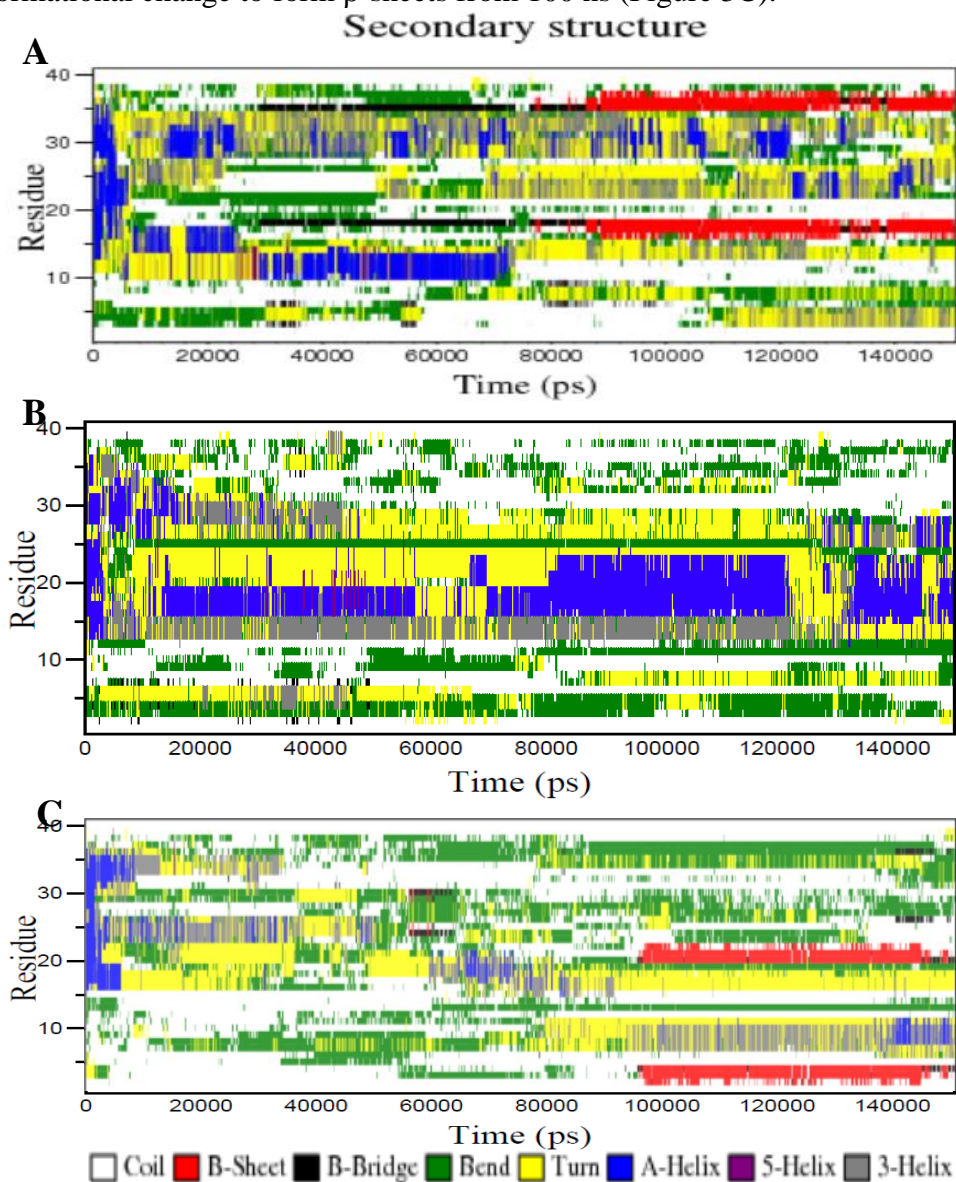
At 0 ns, all the systems started with coiled alpha helical structure as shown in Table 2. As simulation progressed, the alpha helix of A $\beta_{40}$  Only gradually deformed into  $\beta$ -hairpin structure. On the other hand, when A $\beta_{40}$  was treated with ER, even though some unwinding of alpha helix was observed, the structure was deformed less into the  $\beta$ -hairpin structure. In contrast to the treatment with ER, when A $\beta_{40}$  was treated with EOY, similar trend to that of ER-treatment was observed up to 50 ns, but after 100 ns, the protein started to deform in a way similar to that of A $\beta_{40}$  Only.

	0 ns	50 ns	100 ns	150 ns
A $\beta_{40}$ Only				
A $\beta_{40}$ -ER				
A $\beta_{40}$ -EOY				

**Table 2. Deformation of the Structure of A $\beta_{40}$**  The trajectory images were taken for each system at four different time points – 0, 50, 100, and 150 ns – throughout the simulations.

## Secondary Structure Analysis

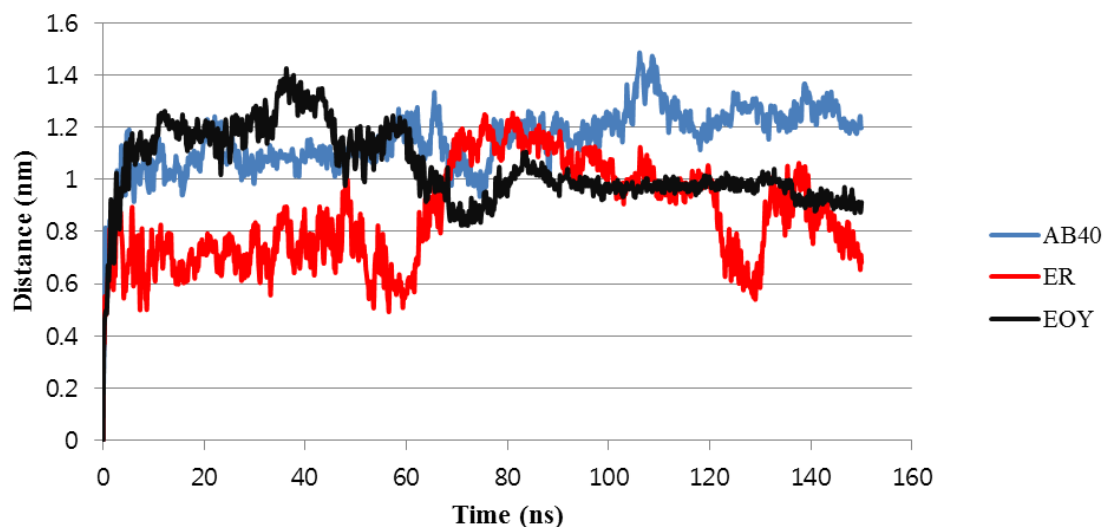
Without any treatment, A $\beta$ <sub>40</sub> started to lose its alpha helical structures (blue), specifically at residue 15-18 and 35-38 (Figure 3A). Starting from approximately 30 ns,  $\beta$ -bridge (black) started to form within those two regions, and by 80 ns  $\beta$ -sheets (red) started to form (Figure 3A). When treated with ER, A $\beta$ <sub>40</sub> maintained blue regions throughout the simulation (Figure 3B), while when treated with EOY, A $\beta$ <sub>40</sub> underwent conformational change to form  $\beta$ -sheets from 100 ns (Figure 3C).



**Figure 3. Secondary structures** Using DSSP, secondary structures were defined for (A) A $\beta$ <sub>40</sub> Only, (B) A $\beta$ <sub>40</sub> with ER, and (C) A $\beta$ <sub>40</sub> with EOY.

### Root Mean Square Deviation (RMSD) Analysis

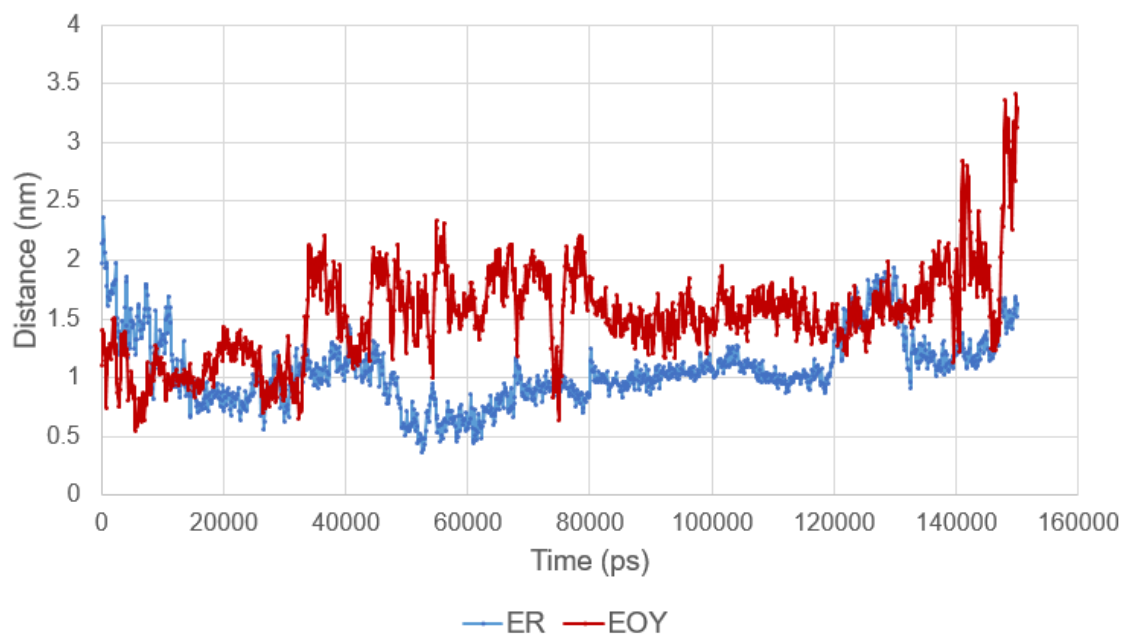
RMSD of atomistic position was calculated to quantify conformation transition of backbone of A $\beta$ <sub>40</sub> during the simulations. Without any drug, A $\beta$ <sub>40</sub> showed RMSD values mostly within the range of 1 – 1.4 nm (Figure 4). RMSD value of this system was 1.152 nm  $\pm$  0.0004 nm. In contrast, when A $\beta$ <sub>40</sub> was treated with ER, the overall RMSD values were lower than those of A $\beta$ <sub>40</sub> Only (Figure 4). Also, maximum value was lower than that of A $\beta$ <sub>40</sub> Only. RMSD value calculated for ER was 0.86 nm  $\pm$  0.002 nm. For EOY treatment, RMSD values were higher than those of A $\beta$ <sub>40</sub> Only up to about 40 ns (Figure 4). Later on, the RMSD values were relatively low compared to A $\beta$ <sub>40</sub> Only, but overall the values were higher than those of ER treatment (Figure 4). The RMSD value for EOY was 1.07 nm  $\pm$  0.05 nm.



**Figure 4. Root mean square deviation of A $\beta$ <sub>40</sub>'s position** For the three different systems, RMSD of the protein's displacement was calculated throughout the simulations, and the three systems were expressed with different colors as indicated in the legend.

### Minimum Distance Calculations

According to Figure 5, despite some fluctuations, the distance between A $\beta$ <sub>40</sub> and ER stayed approximately 1 nm most of the time. Similar to ER, EOY also showed fluctuations in the distance, but it drastically increased to over 2 nm at around 30 ns. Then it stayed at values significantly higher than those of ER and tended to even increase by the end of the simulation.



**Figure 5. Distance between the Drug Molecules and A $\beta$ <sub>40</sub>** Minimum distance between the centers of mass of A $\beta$ <sub>40</sub> and the two drug molecules – ER and EOY – were calculated over the simulation time and plotted with MS Excel. Blue line represents distance between ER and A $\beta$ <sub>40</sub>, and the red represents distance between EOY and the protein.

## CHAPTER 4

### DISCUSSION

#### Structural Deformation of A $\beta$ <sub>40</sub>

Trajectory images taken at various time points showed how A $\beta$ <sub>40</sub> underwent conformational change (Table 2). As expected, when no drug molecule was added to A $\beta$ <sub>40</sub>, it started to actively unfold its  $\alpha$ -helical structure which is indicated by spring-like structure at 0 ns. As time passed, the coiled form became almost not observable, but instead, it began to fold into a hairpin-like loop which is a type of  $\beta$  structure. However, when treated with ER, the protein did not deform as much as A $\beta$ <sub>40</sub> Only did. By 150 ns, the  $\alpha$ -helical structure was almost maintained. This indicates that ER had effect on inhibiting conformational change of A $\beta$ <sub>40</sub>. On the other hand, effect of EOY was questionable. In comparison to A $\beta$ <sub>40</sub> Only, EOY seemed to show some effect in the beginning of the simulation, but at 100 ns, shape of A $\beta$ <sub>40</sub> became similar to that of A $\beta$ <sub>40</sub> Only, which means EOY was not effective anymore from that point. Therefore, it is concluded that ER may be an effective drug candidate while EOY is not.

#### Secondary Structure Analysis of A $\beta$ <sub>40</sub>

To go deeper into observing secondary structure compositions of A $\beta$ <sub>40</sub>, DSSP was used. The DSSP color maps (Figure 3) show different types of secondary structures at forty residues of A $\beta$ <sub>40</sub> throughout the simulations. In Figure 3A, continuous black and red lines are observable at residue 15-18 and 35-38 from 30 ns, indicating that those residues played role in forming  $\beta$  structures. This result agreed with that of the trajectory image observation. For the case of ER treatment, however, the continuation of black and red lines is not observable but rather blue and yellow blocks. This implies that  $\alpha$ -helical and coil structures were maintained throughout the simulation, which was also supported by the trajectories in Table 2. When A $\beta$ <sub>40</sub> was treated with EOY,  $\alpha$ -helical structures were



disappeared even earlier than A $\beta$ <sub>40</sub> Only. Furthermore, EOY-treated A $\beta$ <sub>40</sub> began to form  $\beta$ -sheet structures at residue 1-5 and 20-23 from 100 ns. Like the result of the trajectory image comparison, DSSP analysis result displayed much poorer effect of EOY than ER.

### **Statistical Analysis for A $\beta$ <sub>40</sub> Conformational Change**

Among the three systems, A $\beta$ <sub>40</sub> Only showed the most consistently high RMSD trend (Figure 4), which indicates that A $\beta$ <sub>40</sub> was actively going through conformational change from  $\alpha$ -helix to  $\beta$ -sheet, as shown in trajectories (Table 2). The mean RMSD value of 1.152 was also the highest among the three, and very low SD numerically displayed the consistency. However, ER-treated A $\beta$ <sub>40</sub> showed fluctuations and sudden drops in RMSD values (Figure 4). Furthermore, the mean RMSD value (0.86) was lower than that of A $\beta$ <sub>40</sub> Only. This means ER played a role in preventing movement of the A $\beta$ <sub>40</sub> backbone, which highly possibly led to inhibition of  $\beta$ -sheet structure formation. In the case of EOY, first 40 ns of simulation showed similar trend as the graph for A $\beta$ <sub>40</sub> Only. But, from 60 ns, EOY seemed to reduce the displacement of A $\beta$ <sub>40</sub> backbone shown by relatively low RMSD values compared to A $\beta$ <sub>40</sub> Only. The amount of reduction was not greater than that of ER, but this result was somewhat contradictory to DSSP result for EOY which showed that EOY allowed active conformational change of A $\beta$ <sub>40</sub> from 100 ns (Figure 3). Numerically, the mean RMSD value of EOY was lower than that of A $\beta$ <sub>40</sub> Only but higher than that of ER. Thus, the inhibitory effect of ER was clearly shown through RMSD calculation, but the effect of EOY was doubtable.

### **Distance between Drugs and A $\beta$ <sub>40</sub>**

Distances between the centers of mass of the two compounds and A $\beta$ <sub>40</sub> were calculated to get insights into their interactions during the simulations. Distance between ER and the protein was maintained at relatively low value, which indicated that the two molecules were closely and stably bound to each other (Figure 5). This strong and stable

binding may have affected ER to effectively perform its function of preventing the conformational change of  $A\beta_{40}$ . On the other hand, distance between  $A\beta_{40}$  and EOY was much higher than the case of ER. The plot of EOY, overall, displayed more fluctuations than that of ER, and EOY and  $A\beta_{40}$  were separated even further by the end of the simulation (Figure 5). This trend showed that binding interactions between EOY and  $A\beta_{40}$  were unstable, thus having possibly contributed to the relative ineffectiveness of EOY as a fibrillogenesis inhibitor.

## CHAPTER 5

### CONCLUSIONS

Overall, our study has shown that ER is effective, but EOY is rather ineffective in terms of reducing the harm of  $A\beta_{40}$  monomer by inhibiting its conformational change. Molecular dynamics simulations were run to draw this conclusion. The only structural difference between the two compounds is the type of halogen attached to the xanthene group which refers to the three connected rings; ER has iodine, and EOY has bromine (Figure 1). It is still unsure how the different halogens generate the different outcomes. Our simulation result, however, disagrees with the result of our collaborators, Kwon, et al., who conducted *in vitro* studies on ER and its analogs [2]. According to their study, among five drug candidates, ER and EOY were the best fibrilligenesis inhibitors. Possibly, the difference in the results might have been due to human error or environmental factors in the *in vitro* study or insufficient accuracy in force field development for our simulation. Nevertheless, our study confirmed that halogenation has influence on modulating  $A\beta_{40}$ 's conformational transition and aggregation. Even though more studies are required to understand how different types of halogens contribute to fibrillogenesis inhibition differently, small halogenated compounds might be potential  $A\beta$  modulators. To get an insight into what makes EOY a relatively ineffective inhibitor, more different analysis methods will be utilized in the future. In addition to that, in order to clearly see the effect of halogenation, we will run more simulations using FLN which has the same structure as ER but without any halogens.

## REFERENCES

- [1] Li J, Liu R, Lam KS, Jin L-W, Duan Y. Alzheimer's Disease Drug Candidates Stabilize A- $\beta$  Protein Native Structure by Interacting with the Hydrophobic Core. *Biophys J*. 2011;100(4):1076-1082. doi:10.1016/j.bpj.2010.12.3741.
- [2] Wong HE, Irwin JA, Kwon I. Halogenation Generates Effective Modulators of Amyloid-Beta Aggregation and Neurotoxicity. Lakshmana MK, ed. *PLoS ONE*. 2013;8(2):e57288. doi:10.1371/journal.pone.0057288.
- [3] Aquizzi A, O'Connor T. Protein aggregation diseases: pathogenicity and therapeutic perspectives. *Nat Rev Drug Discov*. 2010; 9(3): 237-248. doi: 10.1038/nrd3050.
- [4] Nowak MW et al. In vivo incorporation of unnatural amino acids into ion channels in *Xenopus* oocyte expression system. *Methods Enzymol*. 1998; 293: 504–529.
- [5] Du WJ et al. Brazilin inhibits amyloid  $\beta$ -protein fibrillogenesis, remodels amyloid fibrils and reduces amyloid cytotoxicity. *Sci Rep*. 2015;5:7992. doi: 10.1038/srep07992.
- [6] Irannejad H, et al. 1,2-Diaryl-2-hydroxyiminoethanones as Dual COX-1 and  $\beta$ -Amyloid Aggregation Inhibitors: Biological Evaluation and In Silico Study. *Chem Biol Drug Des*. 2015; 85(4): 494-503. doi: 10.1111/cbdd.12435.
- [7] Coles, M., Bicknell, W., Watson, A.A., Fairlie, D.P., Craik, D.J. Solution structure of amyloid beta-peptide(1-40) in a water-micelle environment. Is the membrane-spanning domain where we think it is? *Biochemistry*. 1998; 37(31):11064-77.
- [8] Accelrys, Inc. Cerius<sup>2</sup> Modeling Environment (Version 4.10) [Software]. San Diego: Accelrys Software Inc., 2005.
- [9] Bochevarov, A.D., et al. Jaguar: A High-Performance Quantum Chemistry Software Program with Strengths in Life and Materials Sciences. *Int. J. Quantum Chem*. 2013; 113: 2110-2142.
- [10] Morris, G.M., et al. Autodock4 and AutoDockTools4: automated docking with selective receptor flexibility. *J. Comput. Chem*. 2009; 16: 2785-91.

- [11] Lindorff-Larsen K., et al. Improved side-chain torsion potentials for the Amber ff99SB protein force field. *Proteins*. 2010; 78(8):1950-8. doi: 10.1002/prot.22711.
- [12] Mayo, S.L., Olafson, B.D., Goddard, W.A. DREIDING: a generic force field for molecular simulations. *J. Phys. Chem.* 1990; 94(26): 8897-8909.
- [13] Berendsen, H.J.C., Postma, J.P.M., van Gunsteren, W.F., Hermans, J. *Intermolecular Forces*. Pullman, B., Ed. Reidel , Dordrecht. 1981: 331.
- [14] Kabsch, W., Sander, C. Dictionary of protein secondary structure: pattern recognition of hydrogen-bonded and geometrical features. *Biopolymers*. 1983; 22(12): 2577-637.